Peroxisome proliferation in Hansenula polymorpha requires Dnm1p which mediates fission but not de novo formation

Nagotu, Shinisha; Saraya, Ruchi; Otzen, Marleen; Veenhuis, Marten; van der Klei, Ida J.

Published in:
Biochimica et Biophysica Acta-Molecular Cell Research

DOI:
10.1016/j.bbamcr.2007.10.018

Publication date:
2008

Available online at www.sciencedirect.com
ScienceDirect
Biochimica et Biophysica Acta 1783 (2008) 760–769
Biochimica et Biophysica Acta BBA
www.elsevier.com/locate/bbamcr

Peroxisome proliferation in *Hansenula polymorpha* requires Dnm1p which mediates fission but not *de novo* formation

Shirisha Nagotu, Ruchi Saraya, Marleen Otzen, Marten Veenhuis, Ida J. van der Klei *

Molecular Cell Biology, Groningen Biomolecular Sciences and Biotechnology Institute (GBB), University of Groningen, PO Box 14, 9750 AA Haren, The Netherlands

Received 1 August 2007; received in revised form 26 October 2007; accepted 29 October 2007
Available online 12 November 2007

Abstract

We show that the dynamin-like proteins Dnm1p and Vps1p are not required for re-introduction of peroxisomes in *Hansenula polymorpha pex3* cells upon complementation with *PEX3-GFP*. Instead, Dnm1p, but not Vps1p, plays a crucial role in organelle proliferation via fission. In *H. polymorpha DNM1* deletion cells (*dnm1*) a single peroxisome is present that forms long extensions, which protrude into developing buds and divide during cytokinesis. Budding *pex11.dnm1* double deletion cells lack these peroxisomal extensions, suggesting that the peroxisomal membrane protein Pex11p is required for their formation. Life cell imaging revealed that fluorescent Dnm1p-GFP spots fluctuate between peroxisomes and mitochondria. On the other hand Pex11p is present over the entire organelle surface, but concentrates during fission at the basis of the organelle extension in *dnm1* cells.Our data indicate that peroxisome fission is the major pathway for peroxisome multiplication in *H. polymorpha*.

Keywords: Peroxisome; Yeast; Dynamin-like protein; Dnm1p; Pex11p

1. Introduction

Peroxisomes are single membrane bound organelles that are ubiquitously present in eukaryotic cells. Depending on species and environmental conditions, peroxisomes display an unprecedented diversity in protein composition and metabolic functions like fatty acid oxidation and ether–lipid biosynthesis in man, methanol oxidation in methylotrophic yeast and penicillin biosynthesis in fungi [1]. In man inherited disorders are known that result in malfunctioning of peroxisomes and lead to severe abnormalities which often are lethal [2].

Peroxisomes have long been considered to be solely formed by growth and division of pre-existing ones (reviewed in [3–5]). However, recently peroxisome research has made exciting advancements, as the general view that peroxisomes are autonomous organelles – like mitochondria and chloroplasts – has been challenged by data supporting that they may be formed from the endoplasmic reticulum [6]. Also proteins have been identified that are suggested to play a role in peroxisome fission, among others dynamin-like proteins (DLPs), Pex11p and Pex11p-related proteins [5,7].

DLPs are GTPases that play a role in various membrane fusion and fission events. Data from plant, human and yeast cells provide evidence for the involvement of DLPs in peroxisome proliferation as well [8–12]. The baker's yeast genome encodes 3 DLPs, namely Vps1p, Dnm1p and Mgm1p. Vps1p has initially been identified as a protein essential for vacuolar protein sorting [13], but later studies also revealed functions in vacuole fusion and fission events [14] and in peroxisome proliferation [9].

It is well documented that Dnm1p is involved in mitochondrial division and is recruited to the mitochondrial outer membrane by Fis1p [15–18]. Recent observations revealed that both proteins have a dual location and are also localized to peroxisomes, where they play a role in peroxisome proliferation in cells grown at peroxisome-inducing conditions (oleate [8]).

Mgm1p is localized to the mitochondrial inner membrane, where it is involved in mitochondrial fusion [19], but does not function in peroxisome proliferation [9].

* Corresponding author. Tel.: +31 50 3632179; fax: +31 50 3638280.
E-mail address: I.J.van.der.klei@rug.nl (I.J. van der Klei).

0167-4889/$ - see front matter © 2007 Elsevier B.V. All rights reserved.
doi:10.1016/j.bbamcr.2007.10.018

Higher eukaryotes contain a single DLP, designated Dlp1p in mammals and DRP3A in plant [10]. Together with Fis1p, these DLPs are involved in fission of both mitochondria and peroxisomes [11,12].

Pex11p is a peroxisomal membrane protein, whose function so far is mainly speculative. Comparison of genome sequence information of various organisms indicated that most species contain multiple Pex11-like proteins. For instance, *S. cerevisiae* contains Pex11p, Pex25p and Pex27p, whereas PEX11α, β and γ have been identified in mammals [20].

Based on elegant studies performed with mammalian cells, Schrader and colleagues proposed a model predicting that peroxisome fission involves 3 consecutive steps, namely elongation, constriction and fission, and that Pex11p is involved in the first step [11,21,22]. Interestingly, recent data indicated that Pex11β interacts with Fis1p, suggesting that Fis1p, Dlp1p and Pex11β together regulate peroxisome proliferation in mammals [23].

Data that peroxisomes may arise from the ER in yeast and mammals [6,24], raises the question whether peroxisomes are generally formed from the ER with a putative function of DLPs and Pex11p's in e.g. pre-peroxisomal vesicle formation, or whether proliferation of organelles by fission of pre-existing peroxisomes also indeed contributes to a significant extent to the total peroxisome population in induced yeast cells. This study addresses these questions using the methylotrophic yeast *Hansenula polymorpha* as model organism.

2. Materials and methods

2.1. Micro-organisms and growth conditions

The *H. polymorpha* strains used in this study are listed in Table 1. The *dnm1.vps1* and *dnm1.pex3* double mutants were obtained by crossing [25] the *dnm1* and *vps1* or *pex3 (leu1.1)* mutants. Strain *vps1.pex3* was obtained by crossing *pex3 (ura3)* and *vps1*. Diploids were subjected to random spore analysis, and prototrophic segregants were subjected to complementation analysis to determine their genotypes.

Yeast cultures were grown at 37 °C on 1) YPD media containing 1% yeast extract, 1% peptone and 1% glucose, 2) selective media containing 0.67% yeast nitrogen base without amino acids, supplemented with 1% glucose (YND) or 0.5% methanol (YNM) or 3) mineral media (MM) [26] supplemented with 0.5% glucose or 0.5% methanol as carbon sources, and 0.25% ammonium sulphate or 0.25% methylamine as nitrogen sources. When required, amino acids or uracil were added to a final concentration of 30 μg/ml. For growth on agar plates the medium was supplemented with 2% agar. For the selection of resistant transformants YPD plates containing 100 μg/ml zeocin or 100 μg/ml nourseothricin (Invitrogen, Breda, the Netherlands) were used.

For cloning purposes *Escherichia coli* DH5α was used. Cells were grown at 37 °C in LB [27] supplemented with 100 μg/ml ampicillin when required.

2.2. Molecular techniques

Standard recombinant DNA techniques were carried out essentially according to Sambrook et al. [27]. Transformation of *H. polymorpha* cells [28] and site specific integration in the *H. polymorpha* genome [29] were performed as described. DNA modifying enzymes were used as recommended by the suppliers (Roche, Almere, the Netherlands; Fermentas, St. Leon-Rot, Germany). *Pwo* polymerase was used for preparative polymerase chain reactions (PCR). Oligonucleotides were synthesized by Biolegio (Nijmegen,

Table 1
H. polymorpha strains used in this study

Strain	Description	Source/reference
NCYC495	Wild type, *ura3 leu1.1*	[25]
HF246	NCYC495 with one copy integration of plasmid pHI-GFP-SKL, *leu1.1*	[48]
dnm1	DNM1 deletion, ura3	This study
dnm1.GFP-SKL	*dnm1* with integration of plasmid pHipZ4-GFP-SKL	This study
vps1	*VPS1* disruption, *leu1.1*	[20]
vps1.GFP-SKL	*vps1* with integration of plasmid pHipZ4-GFP-SKL	This study
WT.Dnm1-GFP	NCYC495 with one copy integration of plasmid pSNA01	This study
WT.Dnm1-GFP.DsRed-SKL	WT.Dnm1-GFP with integration of plasmid pSNA03	This study
dnm1.Dnm1-GFP	*dnm1* with one copy integration of plasmid pSNA02	This study
dnm1.Dnm1-GFP.DsRed-SKL	*dnm1*.Dnm1-GFP with integration of plasmid pSNA03	This study
dnm1.vps1	Segregant of the cross between *dnm1* and *vps1*	This study
dnm1.vps1.GFP-SKL	*dnm1.vps1* with integration of plasmid pHipZ4-GFP-SKL	This study
dnm1.pex3	Segregant of the cross between *dnm1* and *pex3 (leu)*	This study
dnm1.pex3.Pex3-GFP	*dnm1.pex3* with integration of the plasmid pHipZ5-Pex3-GFP	This study
vps1.pex3	Segregant of the cross between *vps1* and *pex3 (ura3)*	This study
vps1.pex3.Pex3-GFP	*vps1.pex3* with integration of the plasmid pHipZ5-Pex3-GFP	This study
pex3.Pex3-GFP	*PEX3 deletion* with one copy integration of the plasmid pHipZ5-Pex3-GFP	This study
WT.GFP-SKL.DsRed-SKL	NCYC495 with two copy integration of pHipX5-GFP-SKL and one copy integration of pHipZ4-DsRed-SKL	This study
dnm1.Pex11-GFP.DsRed-SKL	*DNM1* with integration of plasmid pEXP-Pex11.GFP and pHipZ4-DsRed-SKL	This study
pex3 (leu)	*PEX3* disruption strain, *ura3*	[49]
pex3 (ura)	*PEX3* deletion strain, *leu1.1*	[33]
pex11	*pex11* deletion, *leu1.1*	[20]
pex11.GFP-SKL	*pex11* with integration of plasmid pHipZ4-GFP-SKL	This study
dnm1.pex11	Segregant of the cross between *dnm1* and *pex11*	This study
dnm1. pex11.DsRed-SKL	*dnm1.pex11* with integration of plasmid pHipZ4-DsRed-T1-SKL	This study
pex11.Pex11-GFP	*pex11* with integration of plasmid pEXP-Pex11-GFP	This study
dnm1.vps1.pex3	*PEX3* deletion in *dnm1.vps1*	This study
dnm1.vps1.pex3.Pex3-GFP	*dnm1.vps1.pex3* with integration of the plasmid pHipZ5-Pex3-GFP	This study

The Netherlands). DNA sequencing reactions were performed at BaseClear (Leiden, The Netherlands) using a LiCor automated DNA-sequencer and dye primer chemistry (LiCor, Lincoln, NB). For DNA sequence analysis, the Clone Manager 5 program (Scientific and Educational Software, Durham, USA) was used.

2.3. Identification of the H. polymorpha VPS1, DNM1 and PEX11 genes

The *H. polymorpha VPS1* gene (GenBank AY780359) and the *H. polymorpha PEX11* gene (GenBank DQ645582) were previously identified (Kuravi, K, unpublished data; [20]). To identify the *H. polymorpha DNM1* gene the BLAST algorithm [30] was used to screen the *H. polymorpha* genome [31] for protein sequences showing similarity to the *S. cerevisiae* Dnm1p. This resulted in a single candidate gene, which was designated *H. polymorpha DNM1*. The *DNM1* ORF consists of 2262 bp that codes for a protein of 753 amino acids with a calculated mass of approximately 84 kDa that shows 61% identity to the *S. cerevisiae* Dnm1p. The nucleotide sequence of *DNM1* is deposited at the GenBank with accession number EF682093.

2.4. Construction of a H. polymorpha dnm1 deletion mutant

A *dnm1* deletion strain was constructed by replacing the genomic region of *DNM1* comprising nucleotides +341 to +1855 by the auxotrophic marker *LEU2*. To this end pDESTDNM1-LEU was made using Gateway® Technology (Invitrogen, Breda, the Netherlands). Two DNA fragments comprising the regions −91 to +340 and 1856 to +2390 of the *DNM1* genomic region were obtained by PCR using respectively primers *att*DNM15F/*att*DNM15R and *att* DNM13F/*att*DNM13R and *H. polymorpha* genomic DNA as a template. The PCR fragments were cloned into the vectors pDONR P4-1R and pDONR P2-P3, respectively, resulting in the entry vectors pENTR DNM1 5′ and pENTR DNM1 3′. Additionally, a DNA fragment comprising the *Candida albicans LEU2* gene was obtained by PCR using primers Entr221_LEUCa_ F and Entr221_LEU-Ca_R and plasmid pB-LEU2Ca as a template. The resulting PCR fragment was recombined into vector pDONR221 resulting in the entry vector pENTR LEU2Ca2. Recombination of the entry vectors pENTR DNM1 5′, pENTR LEU2Ca2 and pENTR DNM1 3′, and the destination vector pDEST R4-R3, resulted in pDESTDNM1-LEU. Subsequently, *H. polymorpha* WT *leu1.1 ura3* cells were transformed with the 3 kb *DNM1* deletion fragment, which was obtained by PCR using primers Dnm15′ and Dnm13′ and pDESTDNM1leu as template. Correct integration was confirmed by PCR and Southern blot analysis. The resulting strain was designated *dnm1*.

2.5. Plasmid construction

Plasmids and primers used in this study are listed in Table 2 and 3. For the construction of plasmid pHI-DsRed-SKL (pSNA03) the 1.2 kb *Nsi*I–*Sma*I fragment from pHipZ4-DsRed-SKL was inserted between the *Nsi*I and *Sma*I of pHI-GFP-SKL. For stable integration of the plasmid into the *H. polymorpha* genome, the plasmid was linearized with *Sac*II in the P_{AOX} region and transformed to various strains.

Plasmid pSNA01 was constructed by amplification of the 1425 bp 3′ end of the *DNM1* gene, lacking the stop codon, using primers DNM1GFPfw and DNM1GFPrv and *H. polymorpha* genomic DNA as template. The resulting PCR product was digested with *Hin*dIII and *Bgl*II, and ligated between the *Hin*dIII and *Bgl*II sites of pANL31 [32]. The resulting plasmid pSNA01 was linearized with *Bst*I to enable integration into the *DNM1* locus of the *H. polymorpha* genome. For the construction of pSNA02 the full length *DNM1* gene, lacking the stop codon, was obtained by PCR using primers DNM1GFP-START and DNM1GFP-NOSTOP. The resulting fragment was digested with *Hin*dIII and

Table 2
Plasmids used in this study

Plasmid	Description	Source or reference
pHipZ5	Plasmid containing *H. polymorpha AMO* promoter and *AMO* terminator regions; zeo^R, amp^R	[28]
pANL31	Plasmid containing *GFP* without start codon; zeo^R, amp^R	[32]
pANL29	pHipZ4 containing P_{AOX}*GFP-SKL*, amp^R, zeo^R	[32]
pHipZ4-DsRed-T1-SKL	Plasmid containing P_{AOX}*DsRed-SKL*, amp^R, zeo^R	[50]
pHipX5-GFP-SKL	Plasmid containing P_{AMO}*GFP-SKL*, kan^R, *LEU2*	[51]
pFEM156	Plasmid containing P_{AOX}*GFP-SKL*, amp^R, *URA3*	[48]
pHipZ5-Pex3-GFP	pHipZ5 containing *PEX3-GFP*; zeo^R, amp^R	This study
pSNA01	pANL31 containing fusion gene between *GFP* and C-terminal part of *DNM1*; zeo^R, amp^R	This study
pSNA02	pHipZ5 containing *DNM1-GFP*; zeo^R, amp^R	This study
pSNA03	Plasmid containing P_{AOX}*DsRed-SKL,* amp^R, *URA3*	This study
pRBG3	Plasmid containing *PEX3* deletion cassette; *URA3*, amp^R	[33]
pSNA04	pRBG3 with *URA3* replaced with Nourseothricin	This study
pBSK-URA3	pBluescript II containing *H. polymorpha URA3*; amp^R	[32]
pB-LEU2Ca	pBluescript II containing *C. albicans LEU2*; amp^R	Lab collection
pHI1	Vector containing *H. polymorpha URA3*; amp^R	[52]
pHI1-*VPS1*	pHI1 plasmid containing *VPS1* disruption cassette	This study
pDONR4 P4-1R	Gateway vector	Invitrogen
pDONR P2-P3	Gateway vector	Invitrogen
pENTR221*URA3*	Gateway vector containing *URA3* marker	Invitrogen
pENTR *LEU2Ca*	Gateway vector containing *LEU2* marker	Invitrogen
pDESTR4-R1	Gateway destination vector	Invitrogen
pDONR-P4-P1r-P_{AMO}	pDONR4 P4-1R containing P_{AMO}	This study
pDONR-P2r-P3-eGFP-T_{AMO}	pDONR P2-P3 containing T_{AMO} and *eGFP*	This study
pDEST-R4-R3-NAT	pDESTR4-R1 containing nourseothricin marker	This study
pENTR DNM1 5′	pDONR4 P4-1R containing 5′ region of *DNM1*	This study
pENTR DNM1 3′	pDONR P2-P3 containing 3′ region of *DNM1*	This study
pDEST *DNM1-LEU*	pDESTR4-R3 containing *DNM1* deletion cassette	This study
pKVK106	pDONR4 P4-1R containing 5′ region of *PEX11*	This study
pKVK107	pDONR P2-P3 containing 3′ region of PEX11	This study
pKVK108	pDESTRA4-R3 containing *PEX11* deletion cassette	This study
pEXP-PEX11-GFP	pDES-R4-R3-NAT containing *PEX11-GFP*	This study

Table 3
Primers used in this study

VPS1KOfw	5′AAAAAGGTACCGGCTGGTCGCCCACAGGAC 3′
VPS1KOrv	5′AAAAAGCATGCTAGGATGAAACATTAATCCAAAC 3′
attDNM15F	5′GGGGACAACTTTGTATAGAAAAGTTGTTTGATCAGCAAGTGGCCAGCTTC 3′
attDNM15R	5′GGGGACTGCTTTTTTGTACAAACTTGGCCAGGCAGATGCAAGAATTCTCC 3′
attDNM13F	5′GGGGACAGCTTTCTTGTACAAAGTGGATTCTTCTTCTCCACCAACCCAGC 3′
attDNM13R	5′GGGGACAACTTTGTATAATAAAGTTGCAAGGCAAGTGATTCCTTATCCAG 3′
Entr221_LEUCa_F	5′GGGGACAAGTTTGTACAAAAAAGCAGGCTGGTGAATCGTTGTTAATGGCC 3′
Entr221_LEUCa_R	5′GGGGACCACTTTGTACAAGAAAGCTGGGTTGGAAACAAGCCCGTGCCCAAG 3′
DNM15F	5′GCAAGTGGCCAGCTTCCCGTATAC 3′
DNM13R	5′CAAGGCAAGTGATTCCTTATCCAG 3′
DNM1GFPfw	5′CCCAAGCTTCTGAGAGCTGAAGAGGAGTTC 3′
DNM1GFrv	5′AGATCTTCCAACAACTTCGCTAATGATAGC 3′
DNM1GFP-START	5′ATGTCGGCATTGCAAGACCT 3′
DNM1GFP-NOSTOP	5′CGCGGATCCAACAACTTCGCTAATGATAGCAGCG 3′
BB-JK-033	5′GGGGACAAGTTTGTACAAAAAAGCAGGCTCCATGGTTTGCGACACGATAACATATCATC 3′
BB-JK-034	5′GGGGACCACTTTGTACAAGAAAGCTGGGTTTAGCACAGAAGACTCGGTCGTGC 3′
PEX11-attB4-fw	5′GGGGACAACTTTGTATAGAAAAGTTGCAGACAGTTATCCAAGGTTTGCGACACG 3′
PEX11-attB1-rev	5′GGGGACTGCTTTTTTGTACAAACTTGCGCAGCAATCCTAGCAACTTG 3′
PEX11-attB2-fw	5′GGGGACAGCTTTCTTGTACAAAGTGGCACTAGCACGACCGAGTCTTC 3′
PEX11-attB3-rev	5′GGGGACAACTTTGTATAATAAAGTTGGGTCGGTAGTCTAGTGGTATG 3′
PEX11-del3.1	5′GGGGACAACTTTGTATAATAAAGTTGGGTCGGTAGTCTAGTGGTATG 3′
PEX11-del3.2	5′ GGTCGGTAGTCTAGTGGTATG 3′
PEX11-4.1	5′GTCCAATCCGCGTTCTCCTC 3′
PEX11-4.2	5′GCGACTGATTCGGCAAGATG 3′
PEX11.fw	5′ ATACTGAAGCTTATGGTTTGCGACACGATAAC 3′
PEX11.rev	5′ACATTGGTCGACTCATAGCACAGAAGACTCGG 3′
pex3-nat-fw	5′ ACCGCGTGAAACTTTATATCG 3′
pex3-nat-rev	5′CAAGGAACGCGATGTATGTT 3′

*Bgl*II and cloned into the *Hin*dIII–*Bgl*II digested pANL31 [32] resulting in the plasmid FL-DNM1-GFP. Subsequently, the *Bam*HI–*Stu*I fragment from the plasmid pHipZ5, containing the P_{AMO} region, was ligated into the *Bam*HI–*Stu*I digested FL-DNM1-GFP plasmid. The resulting plasmid pSNA02 was linearized with *Nar*I in the P_{AMO} region to enable the integration into the *H. polymorpha* genome.

pEXP-PEX11-GFP was constructed using Gateway® Technology. The *PEX11* coding sequence lacking a stop codon was amplified using the primers BB-JK-033 and BB-JK-034 and cloned into the vector pDONR 221. The resulting plasmid pENTR-221-PEX11 was recombined with vectors pDONR-P4-P1r-P_{AMO}, pDONR-P2r-P3-eGFP-T_{AMO} and vector pDEST-R4-R3-NAT. The resulting expression vector pEXP-PEX11-GFP was then linearized by *Nar*I to enable integration into the *H. polymorpha* genome.

For the construction of plasmid pHIPZ5-Pex3-GFP the 2.2 kb *Bam*HI–*Sma*I fragment from pHOR46 was inserted between the *Bam*HI and *Pae*I (blunted) of pHIPZ5. The resulting plasmid was linearized with *Bsi*WI for stable integration into the genome of *H. polymorpha*.

Integration of pHipZ4-GFP-SKL [32] and pHipZ4-DsRed-SKL into the P_{AOX} region of the *H. polymorpha* genome was achieved by transforming *Sph*I-linearized plasmid DNA. Specific integration of pHipX5-GFP-SKL into the *AMO* locus was performed by the transformation of *Bsi*WI-linearized plasmid DNA.

Plasmid pSNA04 was constructed by replacing the *URA3* marker of plasmid pRBG3 [33] with the dominant marker *NAT1* that confers resistance towards nourseothricin. For this replacement, the 1.2 kb *Bgl*II–*Eco*RV fragment from pAG25 [34] was ligated with the 3.7 kb *Bgl*II–*Eco*RV fragment of pRBG3. Subsequently, the deletion cassette obtained by PCR using primers pex3-nat-fw and pex3-nat-rev was used to transform *H. polymorpha dnm1.vps1* cells. Correct integration was confirmed by PCR and Southern blot analysis. The resulting strain was designated *dnm1.vps1.pex3*.

2.6. Morphological analysis

Wide field fluorescence images were made using a Zeiss Axioskop fluorescence microscope [35]. Confocal images and time lapse videos were made using a Zeiss LSM510 confocal laser scanning microscope (CLSM; Zeiss Netherlands bv. Weesp, The Netherlands) [35]. For time lapse videos the temperature of the objective and object slide was kept at 37 °C. Eight *Z*-axis planes were acquired for each time interval. The laser power was set at 50% of its maximum; the AOTF was tuned down to 0.5% [35]. GFP fluorescence was analyzed by excitation of the cells with a 488-nm argon ion laser and detection of fluorescence emission using a bandpass (BP) 500–550 nm filter. DsRed fluorescence was analyzed using a 543-nm helium neon laser and fluorescence was filtered through a BP 565–615 nm filter. Mitochondria were visualized using Mitotracker Deep Red (final concentration of 0.4 μM) that was added to the cultures 15 min before analysis [35]. Mitotracker Deep Red fluorescence was analyzed by excitation of the cells with a 633-nm helium neon laser and fluorescence emission was filtered through a BP 650–710 filter.

For quantitative determination of the number of fluorescent spots per cell, images were prepared using wild field fluorescence microscopy or CLSM. Cells were fixed in 4% formaldehyde in 10 mM potassium phosphate buffer at pH 7.5 for 2 h on ice. The number of fluorescent spots was quantified by counting the spots in non-budding, single cells. In each experiment approximately 300 cells were counted (approx. 2 × 150 cells from 2 independent cultures) using ImageJ software (http://rsb.info.nih.gov/nih-image/). Statistical differences in average numbers were determined using a *Z*-test. The kymogram was prepared using ImageJ.

3. Results

3.1. Peroxisomes may proliferate by fission in WT *H. polymorpha*

In continuation of the ground-breaking recent data that peroxisomes may form in yeast *pex3* mutant cells from the endoplasmic reticulum [35–39], we aimed to investigate whether all organelles derive by this process or whether they also may originate by fission of pre-existing ones and, if so, to which extent the two machineries contribute to the total population of peroxisomes per cell. To analyze this, we integrated two

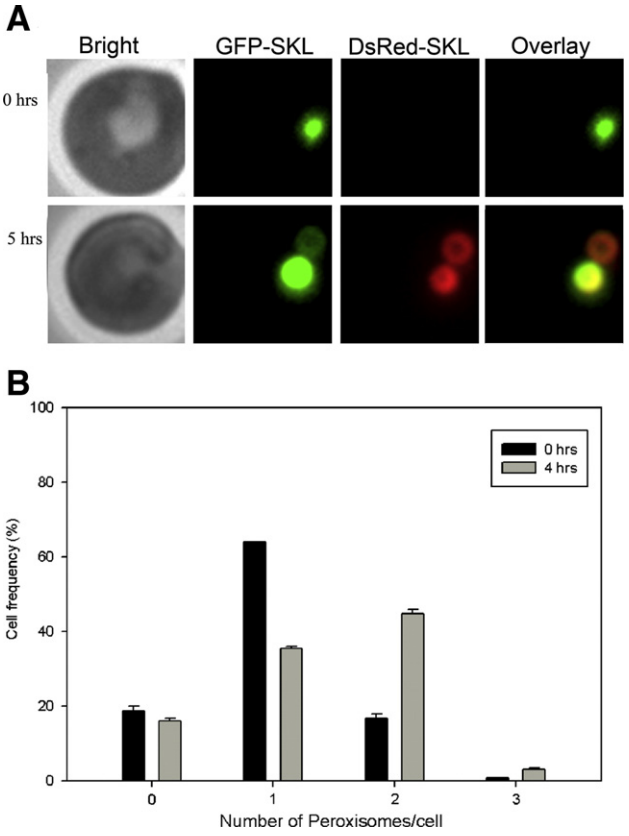

Fig. 1. Fluorescence microscopy of peroxisome proliferation in *H. polymorpha* WT cells. A. Cells grown to the mid-exponential growth phase on glucose/methylamine (T=0 h) contain a single peroxisome marked with GFP-SKL (T=0 h). Five hours (T=5 h) after the shift of these cells to methanol/ammonium sulphate (conditions that induce production of DsRed-SKL concurrently with full repression of GFP-SKL synthesis) the originally present organelle had increased in size due to the uptake of DsRed-SKL and a second organelle had formed by fission. Note that the fluorescence is unevenly distributed over the newly formed organelles. The second organelle contains GFP-SKL under conditions that its synthesis is fully repressed, suggesting that it had derived by fission from the original organelle. Images were prepared using wide field fluorescence microscopy. B. Quantitative analysis of the number of peroxisomes in WT *H. polymorpha* cells. Cells were pre-grown on glucose/methylamine to induce P_{AMO} driven GFP-SKL synthesis (T=0 h). These cells were shifted to methanol/ammonium sulphate medium to repress GFP-SKL synthesis and to induce peroxisome proliferation. The number of green fluorescent peroxisomes per cell was determined using wide field fluorescence microscopy. In bulk of the cells from the initial culture (T=0 h) one green fluorescent peroxisome was detected per cell. After 4 h of cultivation on methanol/ammonium sulphate (T=4 h) the number of cells with two peroxisomes had significantly increased. Virtually all peroxisomes showed green fluorescence (compare to A). Green fluorescent peroxisomes were counted from randomly taken wide field fluorescence microscopy images in 2×150 non-budding cells from 2 independent experiments. The bar represents Standard Error of Mean. The absence of peroxisomes in a portion of the cells is due to peroxisomes that are out of focus.

plasmids into the genome of WT *H. polymorpha* cells, containing P_{AOX}*DsRed-SKL* and P_{AMO}*GFP-SKL*, which allows marking peroxisomes red or green, dependent on the cultivation conditions. Upon introduction of the P_{AOX}*DsRed-SKL* expression cassette cells produce the red fluorescent protein DsRed containing the C-terminal peroxisomal targeting signal SKL under control of the alcohol oxidase promoter (P_{AOX}). P_{AMO}*GFP-SKL* is responsible for the production of peroxisomal green fluorescent protein (GFP-SKL) under control of the amine oxidase promoter (P_{AMO}).

To analyze peroxisome proliferation, cells were pre-grown on glucose/methylamine (to initiate production of GFP-SKL by the amine substrate). Cells from the early-exponential growth phase of this culture characteristically contained a single peroxisome, marked by GFP fluorescence but lacking DsRed fluorescence (Fig. 1A). These cells were harvested by centrifugation, washed and resuspended for 30 min in fresh mineral medium containing ammonium sulphate in the absence of any carbon source. At these conditions P_{AMO} is fully repressed (by ammonium sulphate) and, as established previously, P_{AMO}-induced mRNAs will be fully depleted in this time interval [40]. Then the cells were placed in fresh medium supplemented with methanol/ammonium sulphate to induce P_{AOX} and thus, DsRed-SKL synthesis and peroxisome proliferation concurrent with full repression of GFP-SKL synthesis (by ammonium sulphate). Upon methanol induction, the cells were analyzed by live cell imaging techniques. Time lapse videos (Video 1; stills in Fig. 2A) of an early stage budding yeast cell demonstrated that the pre-existing GFP-marked organelle present in the cells divided to form an additional organelle. This newly formed, smaller organelle rapidly migrated into the developing daughter cell. In a time frame of 23 min, elongation of the peroxisome is observed prior to actual fission. Fission occurred concomitantly with the initiation of bud formation followed by migration of the smaller new organelle into the bud. The fission event is also evident in the kymogram derived from this video and reinforced by the

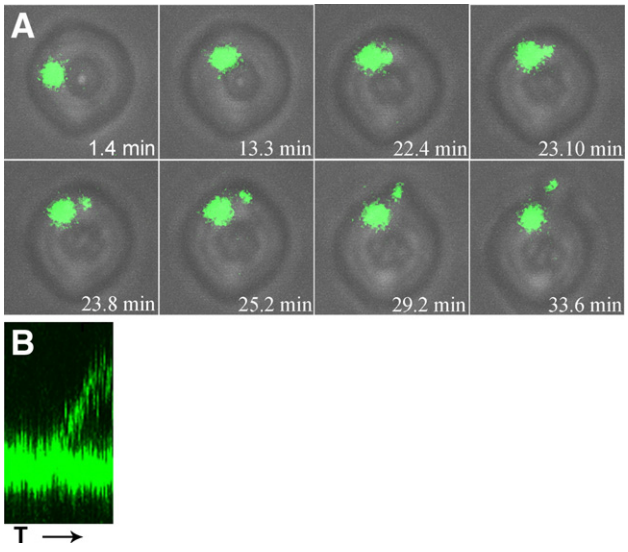

Fig. 2. Peroxisome proliferation in WT *H. polymorpha.* A. Selected images taken from a time lapse video of WT *H. polymorpha* taken by CLSM. The corresponding video (Video 1) is shown in the supplementary data. The depicted cell initially has a single peroxisome which first migrates to the site where a bud is formed, elongates (23 min) and subsequently divides (23.8 min) and the newly formed peroxisome is then inherited by the daughter cell (29.4 min). B shows a kymogram derived from Video 1, which reinforces fission of the original organelle. In this figure the *X*-axis represents the time. At the *Y*-axis the position of fluorescence is shown along a line through the dividing peroxisome.

observation that in the kymogram the original organelle, after fission, is slightly reduced in size (Fig. 2B).

Quantifications were carried out to analyze the increase in peroxisome numbers in identical cultures during the initial hours after the shift of cells to methanol/ammonium sulphate. Prior to the shift bulk of the cells contained a single green fluorescent spot (Fig. 1). But after 4 h of cultivation on methanol/ammonium sulphate the number of cells containing two peroxisomes significantly increased concomitantly with a reduction of cells containing a single organelle (Fig. 1B). At this stage in virtually all organelles green fluorescence was observed (data not shown). Since most organelles showed green fluorescence upon growth at conditions that GFP-SKL synthesis is fully blocked, we conclude that the increase in number is due to fission of the pre-existing (green) ones (Fig. 1A). The matrix content of the original organelles is generally unevenly distributed over the resulting organelles upon fission, suggesting that peroxisome fission is an asymmetrical process (Fig. 1A; Video 1).

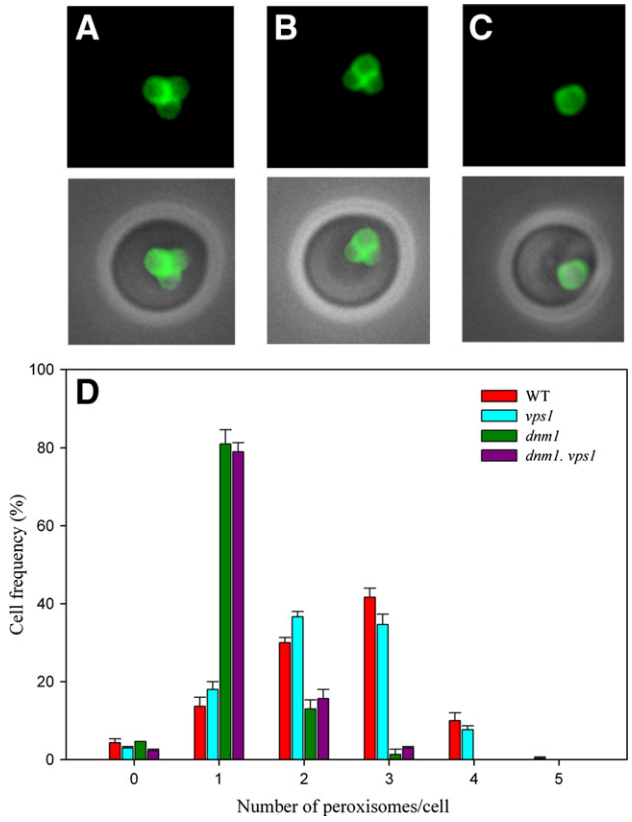

Fig. 3. Peroxisome morphology and numbers in methanol induced cells. Peroxisomes in non-budding WT (A), *vps1* (B) and *dnm1* (C) cells, marked with GFP-SKL. In WT and *vps1* cells the number of peroxisome amounts was generally 3 whereas in *dnm1* cells only a single organelle is observed of enhanced size. Upper row: fluorescence images, second row: merged images of fluorescence and phase contrast pictures. Images were taken by wide field fluorescence microscopy. D shows the quantification of peroxisome numbers in WT, *vps1*, *dnm1* and *dnm1.vps1* double mutant cells, grown on methanol. Organelle numbers were determined by counting from randomly taken CLSM images. For each sample peroxisomes were counted from 2×150 cells from 2 independent experiments. The frequency of cells containing the indicated number of peroxisomes is shown. The bar represents the Standard Error of Mean (SEM).

Table 4
Average number of peroxisomes

Strain	Mean±SEM
WT (HF246)	2.40±0.05
vps1.GFP-SKL	2.25±0.05
dnm1.GFP-SKL	1.11±0.02
dnm1.vps1.GFP-SKL	1.19±0.03

Average numbers of peroxisomes per cell observed in various methanol-grown *H. polymorpha* strains are depicted as mean±SEM. Statistical analysis (*Z*-test) revealed that the differences in average number of peroxisomes in *dnm1*, *dnm1.vps1* cells relative to WT controls were significant (*P*-values<0.005), whereas that of *vps1* cells were not significant. Peroxisomes were marked by GFP-SKL.

3.2. Peroxisome abundance is reduced in dnm1, but not in vps1 cells

Like the *S. cerevisiae* genome, the genome of *H. polymorpha* [31] contains three genes encoding dynamin-like proteins, namely Vps1p, Dnm1p and Mgm1p. Dynamin-like proteins have been indicated to play a role in peroxisome proliferation in *S. cerevisiae*, in particular Dnm1p and Vps1p [8,9]. To analyze the machinery of peroxisome fission in *H. polymorpha*, we have analyzed the function of Dnm1p and Vps1p in an integrated approach.

Cells of constructed *dnm1* and *vps1* mutants and WT controls, all producing GFP-SKL to mark peroxisomes, were grown on peroxisome-inducing methanol media and analyzed by fluorescence microscopy. The data, depicted in Fig. 3, show that WT cells generally contained 3 peroxisomes per cell (average 2.40; Fig. 3A, Table 4). In *vps1* cells, the morphology and average numbers of peroxisomes were largely similar to those of WT cells (average 2.25, Fig. 3B, Table 4). However, in *dnm1* cells the number of peroxisomes was strongly reduced. Most of these cells contained a single enlarged organelle (average 1.11; Fig. 3C, Table 4). Similarly, in *dnm1.vps1* cells generally only one peroxisome was present per cell (average 1.19; Table 4). These data convincingly demonstrates the shift in organelle numbers in *dnm1* and *dnm1.vps1* to predominantly a single organelle per cell relative to WT and *vps1* cells (Fig. 3D).

3.3. Dnm1p is present in dynamic punctuate spots that localize to peroxisomes and mitochondria

Baker's yeast Dnm1p [8] and its mammalian homologue Dlp1p [41] have a dual location on mitochondria and peroxisomes. The location of Dnm1p in *H. polymorpha* was analyzed in cells in which the genomic *DNM1* gene was replaced by *DNM1-GFP* and peroxisomes were labelled by DsRed-SKL. In this strain peroxisome numbers and mitochondrial morphology were like in WT control cells, indicating that the Dnm1p-GFP fusion protein is fully functional (data not shown). Confocal laser scanning microscopy (CLSM) analysis of these cells, in which mitochondria were visualized using Mitotracker Deep Red, revealed that Dnm1p-GFP is present in distinct spots, similar as previously observed in *S. cerevisiae* [15,16]. Bulk of the Dnm1p-GFP spots were localized to mitochondria; however, co-localization of Dnm1p-GFP spots

with DsRed-SKL was also clearly evident indicating that *H. polymorpha* Dnm1p is located on both mitochondria and peroxisomes (Fig. 4A). Remarkably, live cell imaging of such cells strongly suggested that Dnm1p-GFP spots were not permanently localized to peroxisomes or mitochondria, but dynamically moved from peroxisomes to mitochondria and vice versa (Video 2; stills in Fig. 4B).

3.4. Peroxisomes in dnm1 cells form protrusions during budding of cells

Methanol-induced cells of the *H. polymorpha dnm1* strain generally contain a single peroxisome per cell (Fig. 3C,D). Fluorescence analysis of *dnm1* cells revealed an aberrant organelle morphology and inheritance process relative to that of WT cells. During bud formation, the organelles in *dnm1* cells form a protrusion that extends into the bud (Fig. 5A). These protrusions may readily measure over 1 μm and stay intact during subsequent bud development. After bud maturation and subsequent cytokinesis the protrusion is divided resulting in the presence of a small peroxisome in the young bud (Fig. 5A; see also Video 3). We have never observed new-formation of additional organelles suggesting that the presence of peroxisomes in *dnm1* cells solely results from fission.

In budding cells, bulk of the peroxisomes (over 75%; data not shown) normally migrated to the neck between mother cell and bud, as in WT cells [35], prior to forming extensions, suggesting that Dnm1p is not essential for trafficking or positioning of the organelles during vegetative cell reproduction [42,43]. Infrequently, as in WT [35], the organelles remained at the anterior site of budding cells, and in these cases formed relatively long extensions (Fig. 5A,B).

To analyze the site of Dnm1p action, we constructed a *dnm1* strain producing Dnm1p-GFP under control of P_{AMO}. This strain, that also produced DsRed-SKL under control of P_{AOX}, was pre-grown on glucose/ammonium sulphate, conditions at which both the *AOX* and *AMO* promoters are repressed. A shift of such cells to media containing methanol/ammonium sulphate induces peroxisome formation and results in one enlarged peroxisome per cell, characterized by DsRed-SKL, similar as in *dnm1* cells. Methanol/ammonium sulphate-grown cells were subsequently placed in fresh methanol/methylamine media to induce the *AMO* promoter. Within 2 h of cultivation in this media, the first Dnm1p-GFP spots could be observed (Fig. 6A). This initially formed Dnm1p-GFP spot transiently and dynamically localized to the peroxisomal extensions prior to organelle fission. Within a few hours of prolonged cultivation the strain displayed a normal WT phenotype with multiple peroxisomes and Dnm1p-GFP spots per cell.

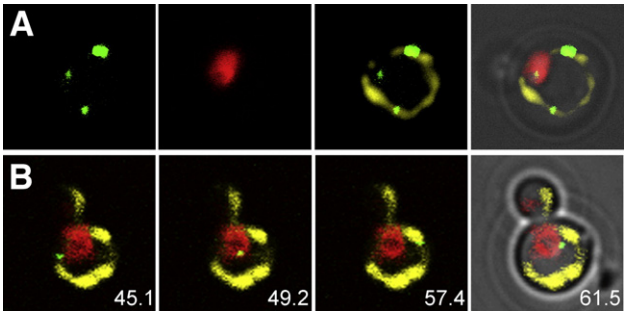

Fig. 4. Dnm1p-GFP spots fluctuate between mitochondria and peroxisomes. A shows the dual location of Dnm1p-GFP to mitochondria and peroxisomes in WT *H. polymorpha*. From left to right: Dnm1p-GFP, DsRed-SKL, Dnm1p-GFP+ Mitotracker Deep Red, merge of all fluorescence images (taken by CLSM) with corresponding phase contrast images. B shows stills of a rapid movie showing the dynamics of Dnm1p-GFP (green spot) localization. The time points of the rapid movie are indicated. Mitochondria are marked by Mitotracker Deep Red (in yellow), peroxisomes by DsRed-SKL (red). The stills demonstrate that within a time frame of 16 s the Dnm1p-GFP spot fluctuates between mitochondria and peroxisomes and vice versa. The corresponding rapid movie is shown in the supplementary data (Video 2).

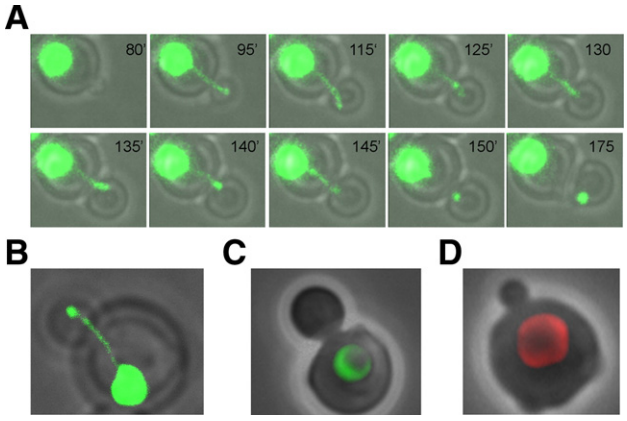

Fig. 5. Inheritance of peroxisomes in *dnm1* cells completes at cytokinesis. A shows stills of a video that visualizes the fission of peroxisomes in methanol-grown *dnm1* cells. The sequence of micrographs shows the organelle elongation and extension into the developing bud and the subsequent fission at the moment of cytokinesis. Peroxisomes are marked by GFP-SKL, the time points of the movie are indicated. The movie was taken by CLSM. The corresponding video is shown in the supplementary data. B exemplifies the strongly elongated organelles observed in *dnm1* cells in which the peroxisome stayed at the anterior site of the cell during budding. C, D show that peroxisomes in *pex11* (C) and *pex11.dnm1* double mutant cells (D) do not form extensions during cell reproduction.

3.5. Pex11p is important for the formation of protrusions at the onset of peroxisome fission

We previously cloned and analyzed the *H. polymorpha PEX11* gene and generated a *PEX11* disruption strain (Kuravi, K; unpublished data). Like that observed for other species, in *H. polymorpha* the absence of Pex11p resulted in strong reduction of peroxisome numbers (generally a single enlarged peroxisome per cell; Fig. 6B). Localization studies in a *pex11* strain producing Pex11p-GFP revealed that this protein is exclusively localized to peroxisomes and generally equally distributed over the organellar surface (Fig. 6C).

To investigate the location of Pex11p in *dnm1* cells, we constructed a *dnm1* strain producing Pex11p-GFP. As shown in Fig. 6D, Pex11p-GFP fluorescence is present at the peroxisomal surface, but concentrates at the region where the protrusion emerges from the organelle.

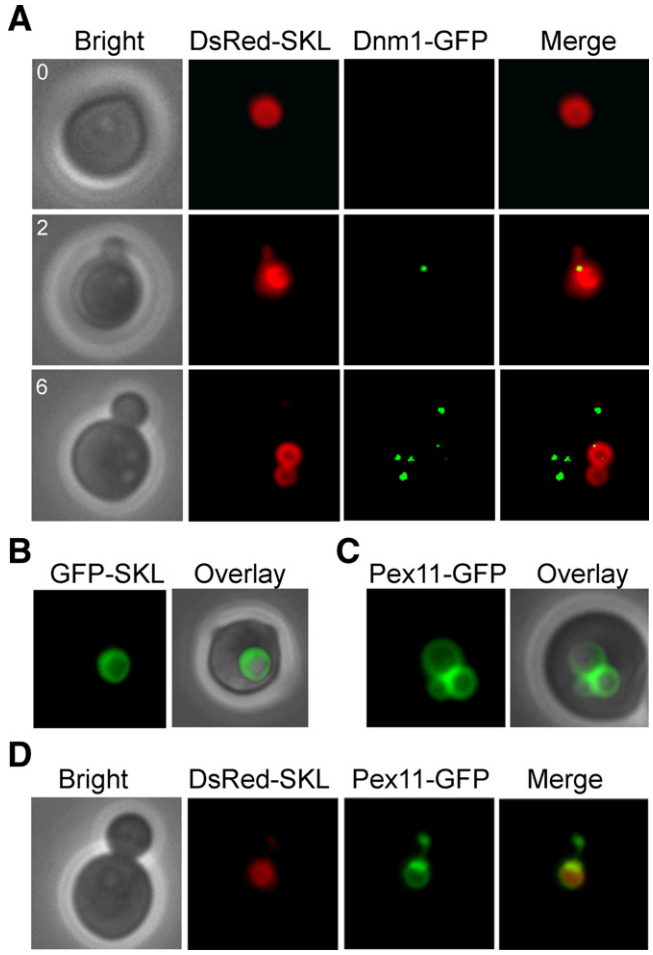

Fig. 6. Dnm1p is required for peroxisome fission. A. Re-introduction of Dnm1p-GFP in a *dnm1* strain lacking *DNM1* (upper row, $T=0$). These cells contain a single organelle marked by DsRed-SKL. Two hours after P_{AMO}-induced synthesis of Dnm1p-GFP in these cells the first green fluorescent spots are observed transiently located at the site of organelle extension (second row, $T=2$ h). Organelle multiplication occurs during subsequent cultivation ($T=6$ h). B. *H. polymorpha pex11* producing GFP-SKL in a non-budding cell illustrating the presence of a single enlarged organelle. C shows the location of Pex11-GFP in a *pex11* strain. GFP fluorescence is present as a rim to peroxisomes in a non-budding *pex11* cell consistent with it being a component of the peroxisomal membrane. D shows that upon P_{AMO}-induced Pex11-GFP synthesis in *dnm1* cells bulk of the Pex11-GFP localizes to the site of organelle extension, marked with DsRed-SKL.

To further establish a role of Pex11p in the formation of peroxisome extensions in *dnm1* cells, we constructed a *dnm1.pex11* double deletion strain. Cells of this strain contain generally one peroxisome (Fig. 5D), similar as in *pex11* or *dnm1* cells (Fig. 5C). Interestingly, as demonstrated in this image (Fig. 5C,D), peroxisome extensions are never observed in these cells during budding.

3.6. Dnm1p and Vps1p are not required for the formation of peroxisomes from the ER

Various recent studies revealed that peroxisomes may be re-introduced in yeast *pex3* (or mammalian *pex16*) cells from the ER after re-introduction of the deleted gene [37–39,44]. This raises the question whether Dnm1p is involved in this peroxisome re-introduction process. To analyze this, we constructed a double mutant *dnm1.pex3*. As expected, cells of this strain were unable to grow on methanol, because of the peroxisome deficiency due to the absence of Pex3p [33]. Subsequently, in these cells we re-introduced *PEX3-GFP* under control of P_{AMO} and monitored the growth of cells on methanol and peroxisome formation.

After pre-cultivation of *dnm1.pex3*.Pex3-GFP cells in glucose–ammonium sulphate, thus repressing P_{AMO}, peroxisomes were undetectable (not shown). After a shift of such cells to methanol/methylamine GFP fluorescence was detected after 1 h of cultivation in a single spot (Fig. 7A) that did not proliferate and remained one organelle per cell also after prolonged cultivation for 16 h. These peroxisomes showed the same elongation phenomena during cell division, indicating that they displayed a *dnm1* phenotype (not shown). The kinetics of peroxisome re-introduction were similar to *pex3*.Pex3-GFP cells, but in these cells normal organelle proliferation was observed after 16 h of cultivation in the methanol/methylamine media (Fig. 7D; [38]). In identical experiments using *vps1.pex3*. Pex3-GFP or *dnm1.vps1.pex3*.Pex3-GFP cells peroxisomes were also formed (Fig. 7B,C).

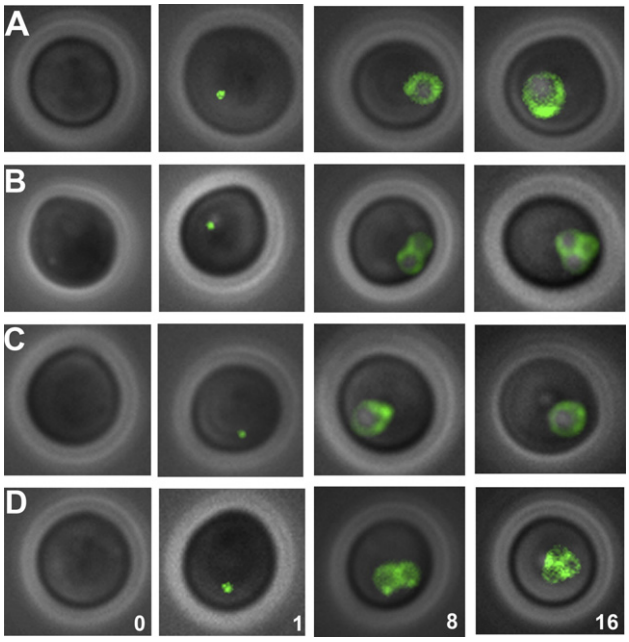

Fig. 7. Dnm1p and Vps1p are not required for re-introduction of peroxisomes in *pex3* cells. Peroxisome re-introduction after induced synthesis of Pex3p.GFP in *dnm1.pex3* (A) *vps1. pex3* (B), *dnm1.vps1.pex3* (C) and *pex3* (D) cells. Peroxisomes appear in all strains (A, B, C) similar as in the *pex3* control strain (D). After induction of Pex3-GFP synthesis, Pex3-GFP fluorescence concentrates into a spot within 1 h (1), followed by the development of peroxisomes. Upon complementation of *pex3* cells or *vps1.pex3* cells multiplication of the organelles is also observed upon prolonged cultivation (shown after 8 and 16 h). Organelle multiplication is not observed upon complementation of *dnm1.pex3* or *dnm1.vps1.pex3* cells (A, C), but the complemented cells exhibit the expected *dnm1* phenotype of organelle enlargement ($T=16$ h) and failure in fission.

From these data we conclude that Dnm1p and Vps1p are not essential for re-introduction of peroxisomes in *H. polymorpha pex3* cells.

4. Discussion

This paper presents evidence for the role of the dynamin-like protein Dnm1p and Pex11p in the peroxisome fission machinery of *H. polymorpha*. Fission as a mode for peroxisome proliferation has been documented before in both yeast and mammals. The data obtained indicated that the peroxisomal and mitochondrial fission machineries share several proteins, among which Dnm1p/DLP1/DRP3A [8,11,45] and Fis1p [22]. Our present data shows that in *H. polymorpha* Dnm1p, but not Vps1p, is required for peroxisome fission. In *S. cerevisiae* however, Vps1p is the main player in peroxisome fission [9] in conjunction with a role for Dnm1p albeit mainly at peroxisome-inducing growth conditions [8]. This illustrates that the peroxisome fission machinery is not fully conserved in yeast.

In contrast to Pex11p, the location of Dnm1p on peroxisomes of *H. polymorpha* is not permanent and not distributed over the entire organelle, as was evident from fast live cell analysis. The observed fluctuation of Dnm1p-GFP spots between organelles of different types has not been demonstrated before. Organelles containing Dnm1p-GFP spots have been observed that lost the GFP fluorescence but regained it at later stages of cultivation. Dnm1p-GPF spots have also been observed in *S. cerevisiae* and most likely represent multimeric protein complexes [15,16].

It has been well documented that the membrane protein Fis1p is essential to recruit Dnm1p to its target organelle. In a recent study, Kobayashi et al. showed that in mammals Fis1p and Pex11p directly interact and, together with Dnm1p, function in peroxisome fission in mammals [23].

Our observation that Pex11p is enriched at the basis of the peroxisomal extensions in budding *dnm1* cells reinforce the data of Kobayashi et al. and suggest that the three proteins (Dnm1p, Fis1p and Pex11p) are indeed dominant players in the peroxisome fission machinery. The single organelles, present in *pex11* cells did not form protrusions and therefore may be unable to divide.

Recently, an alternative mode of peroxisome biogenesis has been elucidated that involves formation of the organelles from the ER [37,39] or, in *Y. lipolytica*, maturation of the ER-derived organelles via immature peroxisome vesicle fusion processes [46]. Also in *H. polymorpha* ER-derived peroxisome biogenesis has been described [35,38]. As yet, it remains unknown to which extent ER-mediated formation and fission contribute to the total peroxisome population per cell. In mammals, Kim et al., concluded from their excellent fluorescence studies that bulk of the organelles is derived from the ER [44].

However, our current data in *H. polymorpha* convincingly demonstrate that Dnm1p and Vps1p are not involved in ER-mediated peroxisome formation. This, together with the finding that in *dnm1* cells generally a single organelle is maintained, led us to conclude that the fission machinery is the main component in peroxisome proliferation in *H. polymorpha* at peroxisome-inducing conditions (methanol). This is in line with the recent observation that in WT *S. cerevisiae* cells peroxisomes also multiply by fission, and not by de novo formation [47]. In conclusion: the suggestion of Kim et al. that peroxisomes predominantly form from the ER may require reconsideration in that the rate of ER-derived biogenesis versus the increase in organelles via fission probably is to a large extent species dependent [44].

Acknowledgements

We thank Richard Baerends, Susan Fekken, Kasinath Kuravi and Elena Kurbatova for their help with the construction of strains. We are grateful to Arjen Krikken for excellent assistance in fluorescence microscopy, image processing and preparation of the figures. We thank Rhein Biotech GmbH, Düsseldorf for access to the *H. polymorpha* genome database. Part of this work was supported by a VENI grant from the Dutch organisation of scientific research (NWO-ALW) to M.O.

Appendix A. Supplementary data

Supplementary data associated with this article can be found, in the online version, at doi:10.1016/j.bbamcr.2007.10.018.

References

[1] I.J. van der Klei, M. Veenhuis, Yeast and filamentous fungi as model organisms in microbody research, Biochim. Biophys. Acta 1763 (2006) 1364–1373.
[2] R.J. Wanders, H.R. Waterham, Peroxisomal disorders I: biochemistry and genetics of peroxisome biogenesis disorders, Clin. Genet. 67 (2005) 107–133.
[3] P.B. Lazarow, Y. Fujiki, Biogenesis of peroxisomes, Annu. Rev. Cell Biol. 1 (1985) 489–530.
[4] P.E. Purdue, P.B. Lazarow, Peroxisome biogenesis, Annu. Rev. Cell Dev. Biol. 17 (2001) 701–752.
[5] M. Yan, N. Rayapuram, S. Subramani, The control of peroxisome number and size during division and proliferation, Curr. Opin. Cell Biol. 17 (2005) 376–383.
[6] H.F. Tabak, D. Hoepfner, A. Zand, H.J. Geuze, I. Braakman, M.A. Huynen, Biochim. Biophys. Acta 1763 (2006) 1647–1654.
[7] S. Thoms, R. Erdmann, Dynamin-related proteins and Pex11 proteins in peroxisome division and proliferation, FEBS J. 272 (2005) 5169–5181.
[8] K. Kuravi, S. Nagotu, A.M. Krikken, K. Sjollema, M. Deckers, R. Erdmann, M. Veenhuis, I.J. van der Klei, Dynamin-related proteins Vps1p and Dnm1p control peroxisome abundance in *Saccharomyces cerevisiae*, J. Cell Sci. 119 (2006) 3994–4001.
[9] D. Hoepfner, M. van den Berg, P. Philippsen, H.F. Tabak, E.H. Hettema, A role for Vps1p, actin, and the Myo2p motor in peroxisome abundance and inheritance in *Saccharomyces cerevisiae*, J. Cell Biol. 155 (2001) 979–990.
[10] S. Mano, C. Nakamori, M. Kondo, M. Hayashi, M. Nishimura, An Arabidopsis dynamin-related protein, DRP3A, controls both peroxisomal and mitochondrial division, Plant J. 38 (2004) 487–498.
[11] A. Koch, M. Thiemann, M. Grabenbauer, Y. Yoon, M.A. McNiven, M. Schrader, Dynamin-like protein 1 is involved in peroxisomal fission, J. Biol. Chem. 278 (2003) 8597–8605.
[12] X. Li, S.J. Gould, The dynamin-like GTPase DLP1 is essential for peroxisome division and is recruited to peroxisomes in part by PEX11, J. Biol. Chem. 278 (2003) 17012–17020.
[13] C.A. Vater, C.K. Raymond, K. Ekena, I. Howald-Stevenson, T.H. Stevens, The VPS1 protein, a homolog of dynamin required for vacuolar protein sorting in *Saccharomyces cerevisiae*, is a GTPase with two functionally separable domains, J. Cell Biol. 119 (1992) 773–786.
[14] C. Peters, T.L. Baars, S. Buhler, A. Mayer, Mutual control of membrane fission and fusion proteins, Cell 119 (2004) 667–678.

[15] W. Bleazard, J.M. McCaffery, E.J. King, S. Bale, A. Mozdy, Q. Tieu, J. Nunnari, J.M. Shaw, The dynamin-related GTPase Dnm1 regulates mitochondrial fission in yeast, Nat. Cell Biol. 1 (1999) 298–304.
[16] A.D. Mozdy, J.M. McCaffery, J.M. Shaw, Dnm1p GTPase-mediated mitochondrial fission is a multi-step process requiring the novel integral membrane component Fis1p, J. Cell Biol. 151 (2000) 367–380.
[17] Q. Tieu, J. Nunnari, Mdv1p is a WD repeat protein that interacts with the dynamin-related GTPase, Dnm1p, to trigger mitochondrial division, J. Cell Biol. 151 (2000) 353–366.
[18] E.E. Griffin, J. Graumann, D.C. Chan, The WD40 protein Caf4p is a component of the mitochondrial fission machinery and recruits Dnm1p to mitochondria, J. Cell Biol. 170 (2005) 237–248.
[19] S. Meeusen, R. DeVay, J. Block, A. Cassidy-Stone, S. Wayson, J.M. McCaffery, J. Nunnari, Mitochondrial inner-membrane fusion and crista maintenance requires the dynamin-related GTPase Mgm1, Cell 127 (2006) 383–395.
[20] J.A. Kiel, M. Veenhuis, I.J. van der Klei, PEX genes in fungal genomes: common, rare or redundant, Traffic 7 (2006) 1291–1303.
[21] A. Koch, G. Schneider, G.H. Luers, M. Schrader, Peroxisome elongation and constriction but not fission can occur independently of dynamin-like protein 1, J. Cell Sci. 117 (2004) 3995–4006.
[22] A. Koch, Y. Yoon, N.A. Bonekamp, M.A. McNiven, M. Schrader, A role for Fis1 in both mitochondrial and peroxisomal fission in mammalian cells, Mol. Biol. Cell 16 (2005) 5077–5086.
[23] S. Kobayashi, A. Tanaka, Y. Fujiki, Fis1, DLP1, and Pex11p coordinately regulate peroxisome morphogenesis, Exp. Cell Res. 313 (2007) 1675–1686.
[24] D. Lay, K. Gorgas, W.W. Just, Peroxisome biogenesis: where Arf and coatomer might be involved, Biochim. Biophys. Acta 1763 (2006) 1678–1687.
[25] P.E. Sudbery, M.A. Gleeson, R.A. Veale, A.M. Ledeboer, M.C. Zoetmulder, *Hansenula polymorpha* as a novel yeast system for the expression of heterologous genes, Biochem. Soc. Trans. 16 (1988) 1081–1083.
[26] J.P. van Dijken, R. Otto, W. Harder, Growth of *Hansenula polymorpha* in a methanol-limited chemostat. Physiological responses due to the involvement of methanol oxidase as a key enzyme in methanol metabolism, Arch. Microbiol. 111 (1976) 137–144.
[27] J. Sambrook, E.F. Fritsch, J. Sambrook, Molecular Cloning : A Laboratory Manual, 2nd ed., Cold Spring Harbor Laboratory, Cold Spring Harbor, N.Y., 1989.
[28] K.N. Faber, P. Haima, W. Harder, M. Veenhuis, G. Ab, Highly-efficient electrotransformation of the yeast *Hansenula polymorpha*, Curr. Genet. 25 (1994) 305–310.
[29] K.N. Faber, G.J. Swaving, F. Faber, G. Ab, W. Harder, M. Veenhuis, P. Haima, Chromosomal targeting of replicating plasmids in the yeast *Hansenula polymorpha*, J. Gen. Microbiol. 138 (1992) 2405–2416.
[30] S.F. Altschul, T.L. Madden, A.A. Schaffer, J. Zhang, Z. Zhang, W. Miller, D.J. Lipman, Gapped BLAST and PSI-BLAST: a new generation of protein database search programs, Nucleic Acids Res. 25 (1997) 3389–3402.
[31] M. Ramezani-Rad, C.P. Hollenberg, J. Lauber, H. Wedler, E. Griess, C. Wagner, K. Albermann, J. Hani, M. Piontek, U. Dahlems, G. Gellissen, The *Hansenula polymorpha* (strain CBS4732) genome sequencing and analysis, FEMS Yeast Res. 4 (2003) 207–215.
[32] A.N. Leao-Helder, A.M. Krikken, I.J. van der Klei, J.A. Kiel, M. Veenhuis, Transcriptional down-regulation of peroxisome numbers affects selective peroxisome degradation in *Hansenula polymorpha*, J. Biol. Chem. 278 (2003) 40749–40756.
[33] R.J. Baerends, K.N. Faber, A.M. Kram, J.A. Kiel, I.J. van der Klei, M. Veenhuis, A stretch of positively charged amino acids at the N terminus of *Hansenula polymorpha* Pex3p is involved in incorporation of the protein into the peroxisomal membrane, J. Biol. Chem. 275 (2000) 9986–9995.
[34] A.L. Goldstein, J.H. McCusker, Three new dominant drug resistant cassettes for gene disruption in *Saccharomyces cerevisiae*, Yeast 15 (1999) 1541–1553.
[35] M. Otzen, A.M. Krikken, P.Z. Ozimek, E. Kurbatova, S. Nagotu, M. Veenhuis, I.J. van der Klei, In the yeast *Hansenula polymorpha*, peroxisome formation from the ER is independent of Pex19p, but involves the function of p24 proteins, FEMS Yeast Res. 6 (2006) 1157–1166.
[36] Y.Y. Tam, A. Fagarasanu, M. Fagarasanu, R.A. Rachubinski, Pex3p initiates the formation of a preperoxisomal compartment from a subdomain of the endoplasmic reticulum in *Saccharomyces cerevisiae*, J. Biol. Chem. 280 (2005) 34933–34939.
[37] A. Kragt, T. Voorn-Brouwer, M. van den Berg, B. Distel, Endoplasmic reticulum-directed Pex3p routes to peroxisomes and restores peroxisome formation in a *Saccharomyces cerevisiae* pex3Delta strain, J. Biol. Chem. 280 (2005) 34350–34357.
[38] G.J. Haan, R.J. Baerends, A.M. Krikken, M. Otzen, M. Veenhuis, I.J. van der Klei, Reassembly of peroxisomes in *Hansenula polymorpha* pex3 cells on reintroduction of Pex3p involves the nuclear envelope, FEMS Yeast Res. 6 (2006) 186–194.
[39] D. Hoepfner, D. Schildknegt, I. Braakman, P. Philippsen, H.F. Tabak, Contribution of the endoplasmic reticulum to peroxisome formation, Cell 122 (2005) 85–95.
[40] H.R. Waterham, V.I. Titorenko, G.J. Swaving, W. Harder, M. Veenhuis, Peroxisomes in the methylotrophic yeast *Hansenula polymorpha* do not necessarily derive from pre-existing organelles, EMBO J. 12 (1993) 4785–4794.
[41] Y. Yoon, K.R. Pitts, M.A. McNiven, Mitochondrial division: new partners in membrane pinching, Mol. Biol. Cell 12 (2001) 2894–2905.
[42] A. Fagarasanu, M. Fagarasanu, G.A. Eitzen, J.D. Aitchison, R.A. Rachubinski, The peroxisomal membrane protein Inp2p is the peroxisome-specific receptor for the myosin V motor Myo2p of *Saccharomyces cerevisiae*, Dev. Cell 10 (2006) 587–600.
[43] M. Fagarasanu, A. Fagarasanu, Y.Y. Tam, J.D. Aitchison, R.A. Rachubinski, Inp1p is a peroxisomal membrane protein required for peroxisome inheritance in *Saccharomyces cerevisiae*, J. Cell Biol. 169 (2005) 765–775.
[44] P.K. Kim, R.T. Mullen, U. Schumann, J. Lippincott-Schwartz, The origin and maintenance of mammalian peroxisomes involves a de novo PEX16-dependent pathway from the ER, J. Cell Biol. 173 (2006) 521–532.
[45] M. Schrader, Shared components of mitochondrial and peroxisomal division, Biochim. Biophys. Acta 1763 (2006) 531–541.
[46] T. Guo, Y.Y. Kit, J.M. Nicaud, M.T. Le Dall, S.K. Sears, H. Vali, H. Chan, R.A. Rachubinski, V.I. Titorenko, Peroxisome division in the yeast *Yarrowia lipolytica* is regulated by a signal from inside the peroxisome, J. Cell Biol. 162 (2003) 1255–1266.
[47] A.M. Motley, E.H. Hettema, Yeast peroxisomes multiply by growth and division, J. Cell Biol. 178 (2007) 399–410.
[48] R. van Dijk, K.N. Faber, A.T. Hammond, B.S. Glick, M. Veenhuis, J.A. Kiel, Tagging *Hansenula polymorpha* genes by random integration of linear DNA fragments (RALF), Mol. Genet. Genomics 266 (2001) 646–656.
[49] R.J.S. Baerends, S.W. Rasmussen, R.E. Hilbrands, M. van der Heide, K.N. Faber, P.T. Reuvekamp, J.A. Kiel, J.M. Cregg, I.J. van der Klei, M. Veenhuis, The *Hansenula polymorpha* PER9 gene encodes a peroxisomal membrane protein essential for peroxisome assembly and integrity, J. Biol. Chem. 271 (1996) 8887–8894.
[50] I. Monastyrska, M. van der Heide, A.M. Krikken, J.A. Kiel, I.J. van der Klei, M. Veenhuis, Atg8 is essential for macropexophagy in *Hansenula polymorpha*, Traffic 6 (2005) 66–74.
[51] P. Ozimek, K. Lahtchev, J.A. Kiel, M. Veenhuis, I.J. van der Klei, *Hansenula polymorpha* Swi1p and Snf2p are essential for methanol utilization, FEMS Yeast Res. 4 (2004) 673–682.
[52] J.A. Kiel, R.E. Hilbrands, I.J. van der Klei, S.W. Rasmussen, F.A. Salomons, M. van der Heide, K.N. Faber, J.M. Cregg, M. Veenhuis, *Hansenula polymorpha* Pex1p and Pex6p are peroxisome-associated AAA proteins that functionally and physically interact, Yeast 15 (1999) 1059–1078.